

Supporting Information

Constructing of triple sequential junction for efficient separation of photogenerated charges in photocatalysis

Chun Li,^{‡a} Xia Yang,^{‡a} Xuebing Chen,^a Jifa Liu,^a Jing Zhang,^{*a} Fangfang Wang,^a

Rengui Li,^{*b} Yang Qu,^c Liqiang Jing^c

^a School of Chemistry and Materials Science, Liaoning Shihua University, No.1 West Dandong Road, Wanghua District, Fushun 113001, China.

^b State Key Laboratory of Catalysis, Dalian National Laboratory for Clean Energy, and The Collaborative Innovation Center of Chemistry for Energy Materials (iChEM), Dalian Institute of Chemical Physics, Chinese Academy of Sciences, Zhongshan Road 457, Dalian 116023, China.

^c Key Laboratory of Functional Inorganic Materials Chemistry, Heilongjiang University, Ministry of Education School of Chemistry and Materials Science, Harbin 150080, China.

*Email: jingzhang_dicp@live.cn, rgli@dicp.ac.cn

[‡]These authors contributed equally to this work.

Materials and methods

Materials

Tetrabutyl titanate (TBOT, 98%), triethanolamine (TEOA, 78%), nitric acid (HNO₃), titanium tetrachloride (TiCl₄, 98%), isopropyl alcohol (99.7%), methanol (99.5%), and ethanol absolute (99.7%) were purchased from Sinopharm Chemical Reagent Co., Ltd (China). All the above reagents were used without further purification. Deionized water was used throughout all the experiment.

Preparation of anatase/rutile heterophase (A_{ns}/R), rutile/rutile homophase (R_{ns}/R), and triple sequential junction (A_{ns}-R_{ns}/R)

For preparation of the A_{ns}/R, R_{ns}/R, and A_{ns}-R_{ns}/R, the rutile TiO₂ nanorods (denoted as R) and anatase TiO₂ nanoparticles (denoted as A_{ns}) were synthesized firstly. The R nanorods were synthesized through a modified one-step hydrothermal treatment of TiCl₄ solution.¹ The preparation procedure of A_{ns} was analogous to the gel-sol method described previously.² The particle size of A_{ns} can be tuned to be around 7 nm, 15 nm, and 25 nm, respectively when PH value is 0.9, 4.2, and 7.8. In the following synthetic procedure, A_{ns} denote as the anatase particle with around 7 nm unless otherwise specified.

In a typical synthesis of A_{ns}/R, R_{ns}/R, and A_{ns}-R_{ns}/R, 5 wt% A_{ns} and 95 wt% R were thoroughly mixed and were dispersed in 50 ml isopropyl alcohol, and then ultrasonic treatment for 2 h to form a homogeneous suspension. After removing the isopropyl alcohol via evaporation at 90 °C under continuous stirring, the precipitate (A_{ns}/R-p) was collected (Scheme S1) and calcined at relevant temperatures for 4 h and the heating rate was 10 °C/min. For the calcination of A_{ns}/R-p at 400 °C, the A_{ns}/R heterophase junction sample was obtained, while the homophase junction R_{ns}/R was obtained for the calcination temperature is at 700 °C because anatase A_{ns} was transformed completely into rutile R_{ns}. The triple sequential junction (A_{ns}-R_{ns}/R) was fabricated when the A_{ns}/R-p was calcined at the range of 500-620 °C. The A_{ns}-R_{ns}/R samples were donated as A_{ns}(x)-R_{ns}(y)/R according to the content of A_{ns} or R_{ns}.

To investigate the effect of TiO₂ particle size on the formation of triple sequential junction, the anatase TiO₂ nanoparticles in the diameters of around 15 nm and 25 nm were also fabricated on R nanorods to form anatase/rutile heterophase junction, and then a following calcination process was introduced for fabricating triple sequential junction, which is similar as those procedure for A_{ns}-R_{ns}/R with 7 nm of A_{ns}.

Characterization

The powder X-ray diffraction (XRD) patterns were recorded on a Rigaku RotaflexRu-200 B diffractometer using Cu K α radiation ($\lambda=1.5418 \text{ \AA}$) with a speed of 5 °/min in the range from 20 to 75 °. Raman spectra excited at 532 nm were recorded on a home-assembled UV Raman spectrograph (DL-3 UV Raman spectroscopy with operando system) with spectral resolution of 2 cm⁻¹. The particle size and morphology of the samples were examined by scanning electron microscopy (SEM, FEI, Quanta 200 F). The Brunauer-Emmett-Teller (BET) surface area was determined by nitrogen adsorption-desorption isotherms using a NOVA 4200e surface area analyzer. UV-vis diffuse reflectance spectra (UV-vis DRS) were recorded on a JASCOV-650 UV-vis spectrophotometer.

Photoelectrochemical measurement was performed with Ivium Vertex One in a three-electrode cell with sample coated on 1 cm² FTO (1 mg·cm⁻²) as the working electrode, Ag/AgCl electrode (saturated KCl) as the reference electrode, Pt plate as the counter electrode. Unless specific statement, the potentials in this work are all referred to Ag/AgCl (saturated KCl). The working electrode was prepared by dropping 100 μ L dispersion solution onto a piece of 1 cm² FTO glass, and then the electrode was allowed dried in air overnight. The dispersion solution was prepared by ultrasonically mixing 10 mg sample powder, 50 μ L 5 wt% Nafion solution (DuPont) and 1 ml isopropanol in a sealed centrifugal tube for 30 min. Mott-Schottky plots were measured at 1000 Hz from 1 V to -1 V in 0.1 M Na₂SO₄ aqueous electrolyte. For open circuit potential (OCP) decay measurements, the OCP was monitored in 0.1 M Na₂SO₄ aqueous electrolyte under a 300 W Xenon lamp, and the light interruption was performed using a plate

composed of one layer of tinfoil and one layer of print paper, which was quickly put in front of the Xenon lamp when the OCP under light was stable. Electrochemical impedance spectroscopy (EIS) was measured at open circuit potential in 0.01 M (1/1) $\text{K}_3\text{Fe}(\text{CN})_6/\text{K}_4\text{Fe}(\text{CN})_6$ and 0.1 M Na_2SO_4 from 100 kHz to 100 mHz.

The surface photovoltage spectroscopy (SS-SPS) and transient-state surface photovoltage (TS-SPV)

The surface photovoltage spectroscopy (SS-SPS) was carried on an assembled instrument with a photovoltaic cell. The samples were pressed on the middle of two ITO electrodes ($d = 1.2$ mm, resistivity: $8\text{-}12 \Omega\cdot\text{cm}^{-2}$, Sigma-Aldrich, USA). The photovoltage signal of samples was amplified by lock-in amplifier (SR830 DSP, Stanford research systems, USA). The monochromatic light was a light source provided by 500 W xenon lamp (CHF-XM-500W, Beijing Perfect Light Co., China) coupling with a grating monochromator (Omni- λ 3007, Zolix, China). There was no external bias applied.

Transient-state surface photovoltage (TS-SPV) measurements for samples were measured through the procedures that the sample chamber applying an (Indium-Tin Oxide) ITO glass as top electrode and a steel substrate as bottom electrode, and a 10 μm thick mica spacer was placed between the ITO glass and the sample to decrease the space charge region at the ITO-sample interface as previous report. The samples were excited by a radiation pulse of 532 nm with 10 ns width from the second harmonic of a neodymium-doped yttrium aluminum garnet (Nd:YAG) laser (Lab-130-10H, Newport, Co.). Intensity of the pulse was measured by a high-energy pyroelectric sensor (PE50BF-DIF-C, Ophir Photonics Group). The signals were amplified with a preamplifier and then registered by a 1 GHz digital phosphor oscilloscope (DPO 4104B, Tektronix). The TS-SPV measurements were performed in air atmosphere and at room temperature.

Photocatalytic reaction

The photocatalytic activity of A_{ns}/R , or R_{ns}/R , or $A_{ns}-R_{ns}/R$ was investigated through the photocatalytic H_2 evolution from methanol/water solutions with Pt as a co-catalyst. Experiments of photocatalytic reaction were carried out in a Pyrex reaction cell, connected to a closed gas circulation and a vacuum system. A 300 W top-irradiated Xenon lamp was used as a light source. Typically, 0.05 g of catalyst was suspended in an aqueous solution containing H_2O (90 mL) and CH_3OH (10 mL). Pt (0.2 wt%) was in-situ photodeposited on the TiO_2 catalysts from precursor H_2PtCl_6 under irradiation. Before irradiation, the system was vacuumed for 30 min through the vacuum pump to remove any dissolved oxygen and put the reactor in an anaerobic state. The amount of evolved H_2 was determined by an on-line gas chromatograph (GC7900 gas chromatography system, Shanghai Techcomp. LTD, Ar carrier).

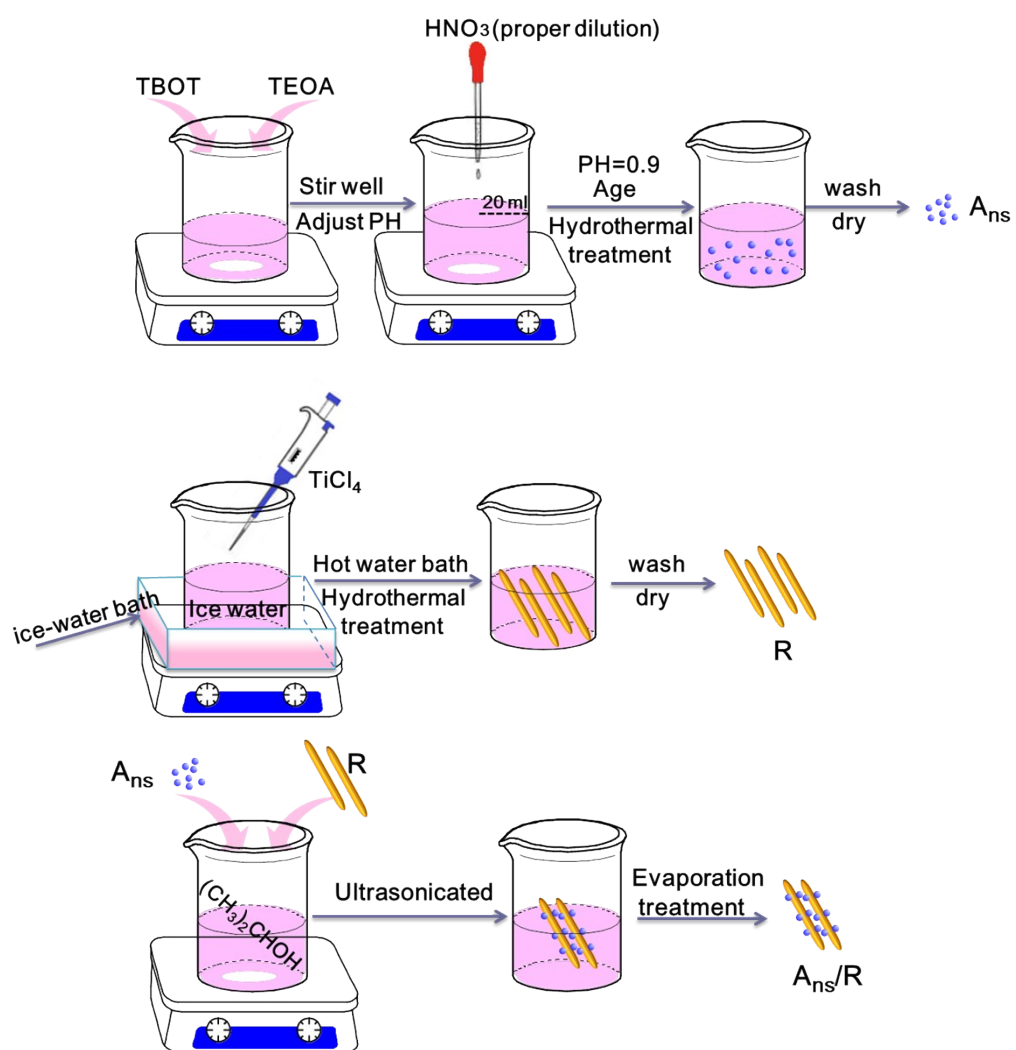
Reference

- 1 W. W. Fu, G. D. Li, Y. Wang, S. J. Zeng, Z. J. Yan, J. W. Wang, S. G. Xin, L. Zhang, S. W. Wu and Z. T. Zhang, *Chem. Commun.*, 2018, **54**, 58.
- 2 J. Zhang, X. B. Chen, Y. Bai, C. Li, Y. Gao, R. G. Li, and C. Li, *J. Mater. Chem. A*, 2019, **7**, 10264.

Table of Contents

	Captions
Scheme S1	Schematic illustration of preparing fairly uniform A_{ns} nanoparticles, R substrates and their complex A_{ns}/R .
Fig. S1	SEM image of (a) A_{ns} , (b) TEM image of A_{ns} (c) SEM image of R_{ns} , and (d) R.
Fig. S2	(a) XRD patterns, (b) Raman spectra and (c) Phase composition of A_{ns} calcined at various temperatures, (d) XRD patterns of R and R-700°C.
Fig. S3	SEM images of (a) R and (b) R-700°C.
Fig. S4	SEM images of (a) A_{ns}/R , (b) $80A_{ns}-20R_{ns}/R$, (c) $23A_{ns}-77R_{ns}/R$ and (d) R_{ns}/R samples.
Fig. S5	Stability of photocatalytic H_2 evolution on (a) $80A_{ns}-20R_{ns}/R$, (b) $48A_{ns}-52R_{ns}/R$, and (c) $23A_{ns}-77R_{ns}/R$ samples
Fig. S6	TEM images of A_{ns} anatase nanoparticles with (a) around 7 nm, (b) around 15 nm, and (c) around 25 nm
Fig. S7	The influence of particle size of A_{ns} in the $A_{ns}-R_{ns}/R$ on the photocatalytic hydrogen evolution
Scheme S2	Schematic illustration of the morphology variations for the prepared samples.

Supplementary Figures



Scheme S1 Schematic illustration of preparing fairly uniform A_{ns} nanoparticles, R substrates and their complex A_{ns}/R .

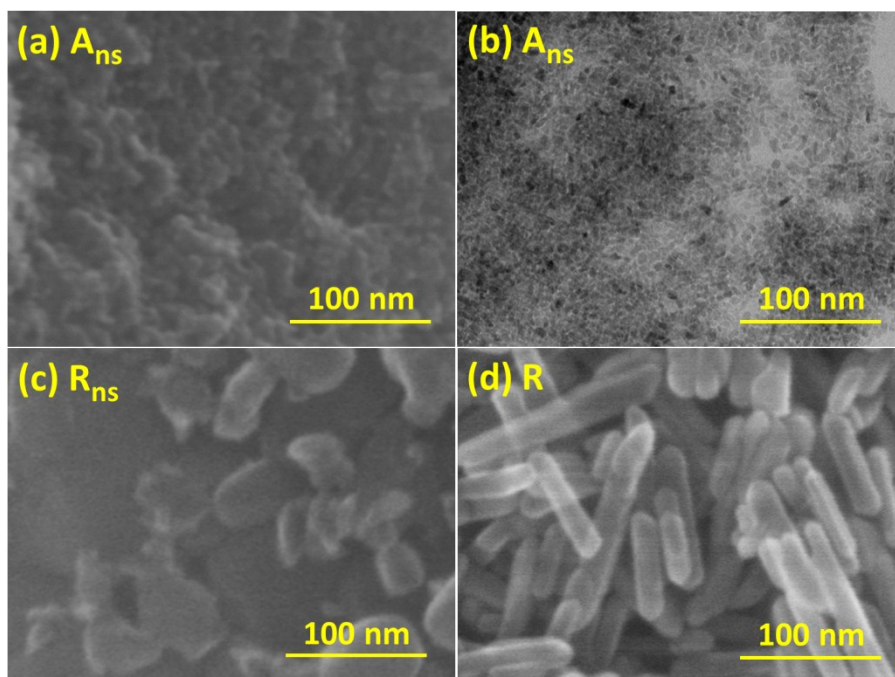


Fig. S1 SEM image of (a) A_{ns} , (b) TEM image of A_{ns} (c) SEM image of R_{ns} , and (d) R .

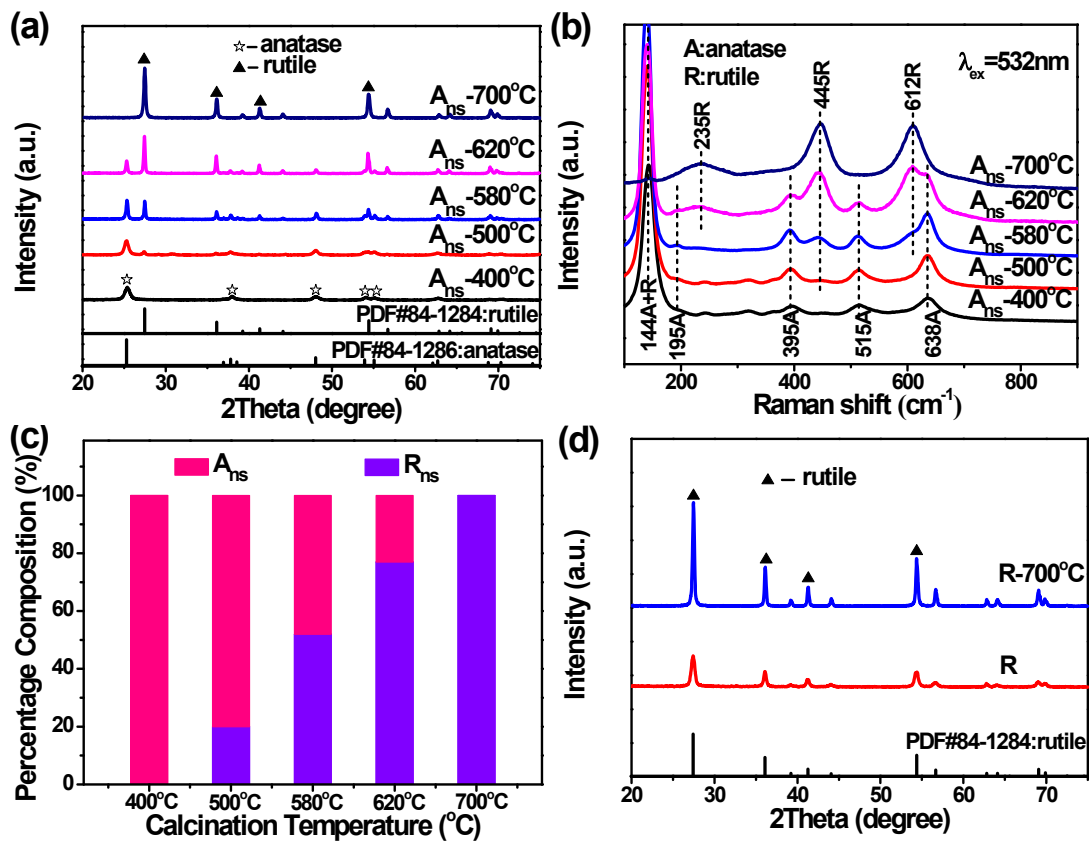


Fig. S2 (a) XRD patterns, (b) Raman spectra and (c) Phase composition of A_{ns} calcined at various temperatures, (d) XRD patterns of R and R-700°C.

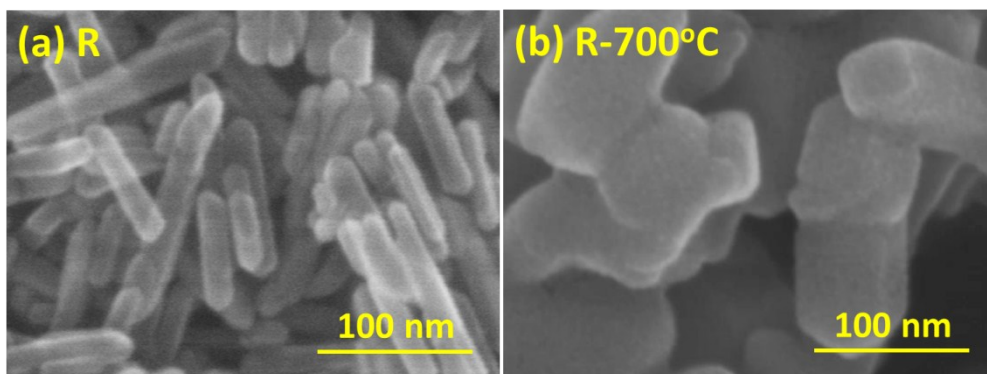


Fig. S3 SEM images of (a) R and (b) R-700°C.

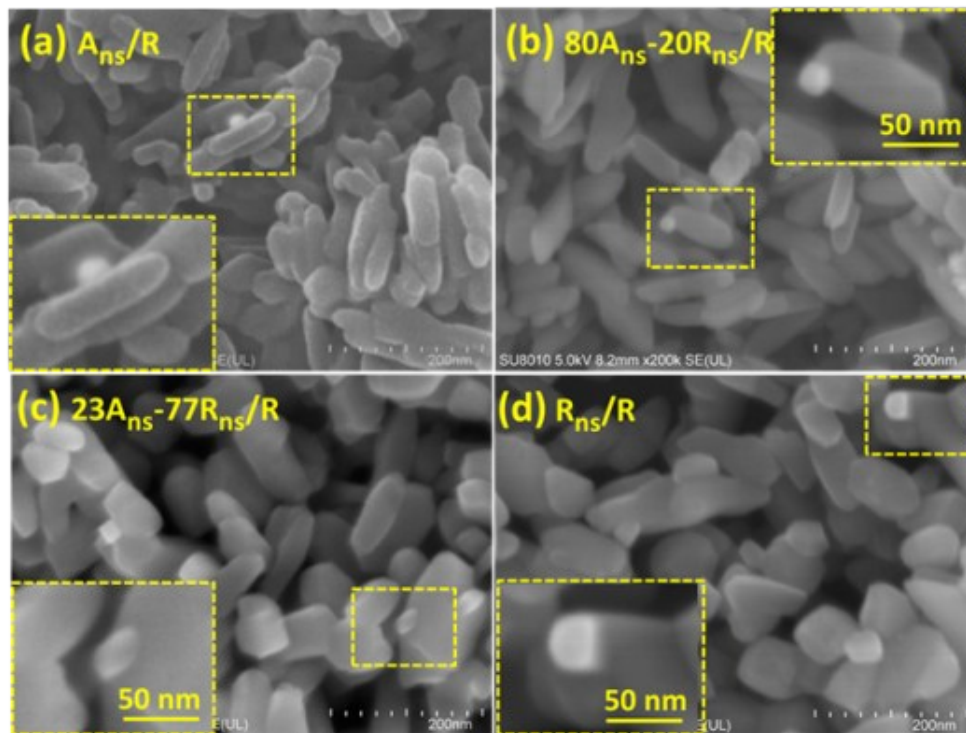


Fig. S4 SEM images of (a) A_{ns}/R , (b) $80A_{ns}-20R_{ns}/R$, (c) $23A_{ns}-77R_{ns}/R$ and (d) R_{ns}/R samples.

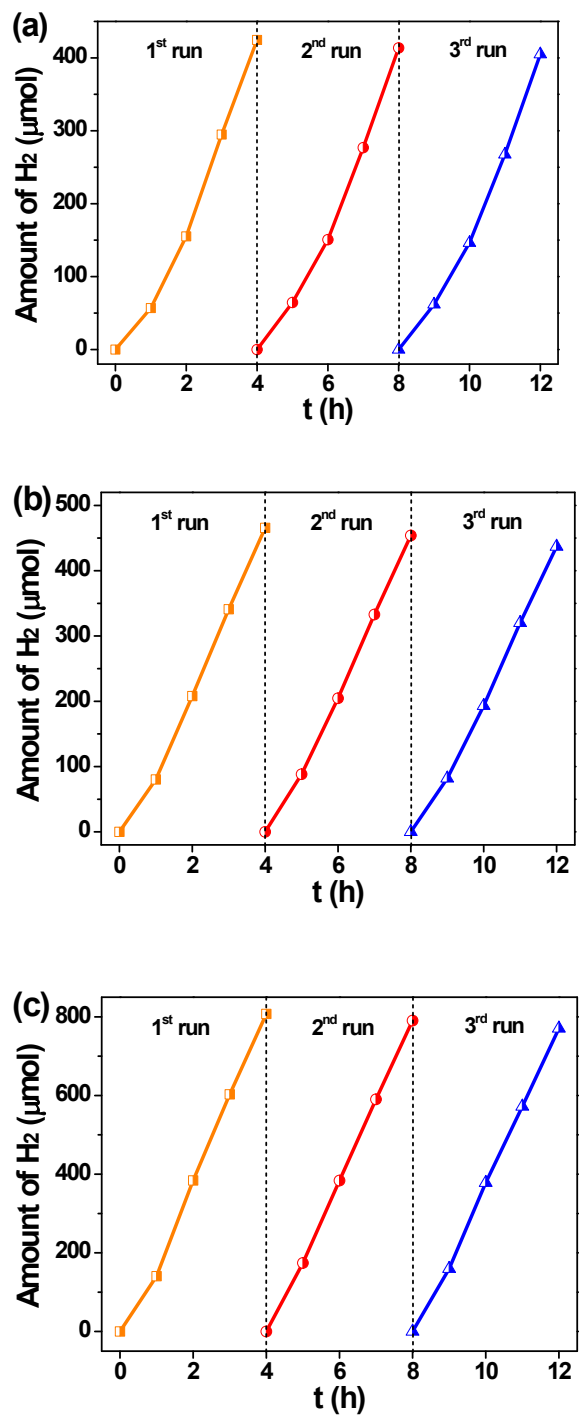


Fig. S5 Stability of photocatalytic H₂ evolution on (a) 80A_{ns}-20R_{ns}/R, (b) 48A_{ns}-52R_{ns}/R, and (c) 23A_{ns}-77R_{ns}/R samples.

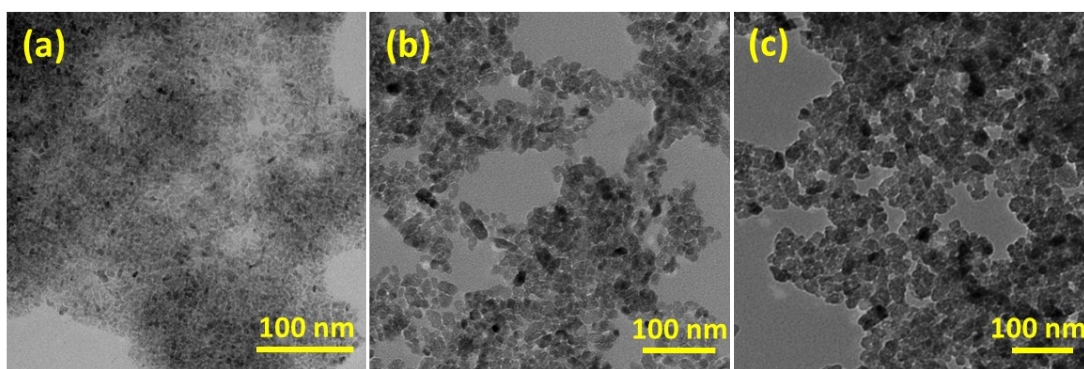


Fig. S6 TEM images of A_{ns} anatase nanoparticles with (a) around 7 nm, (b) around 15 nm, and (c) around 25 nm

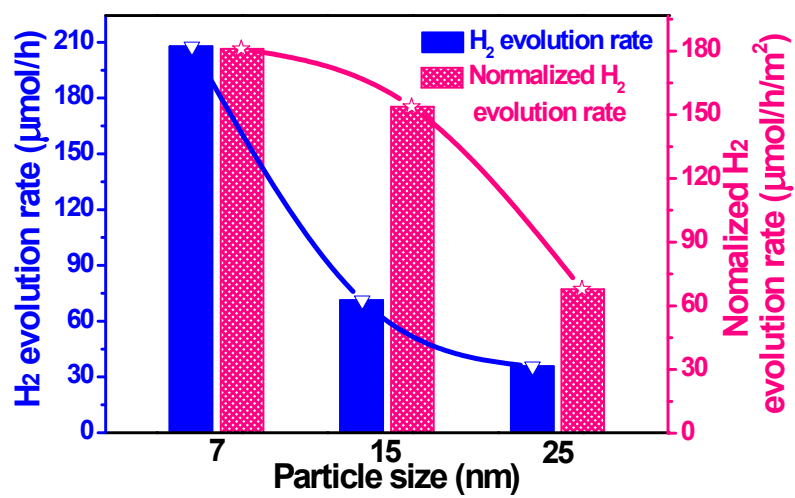
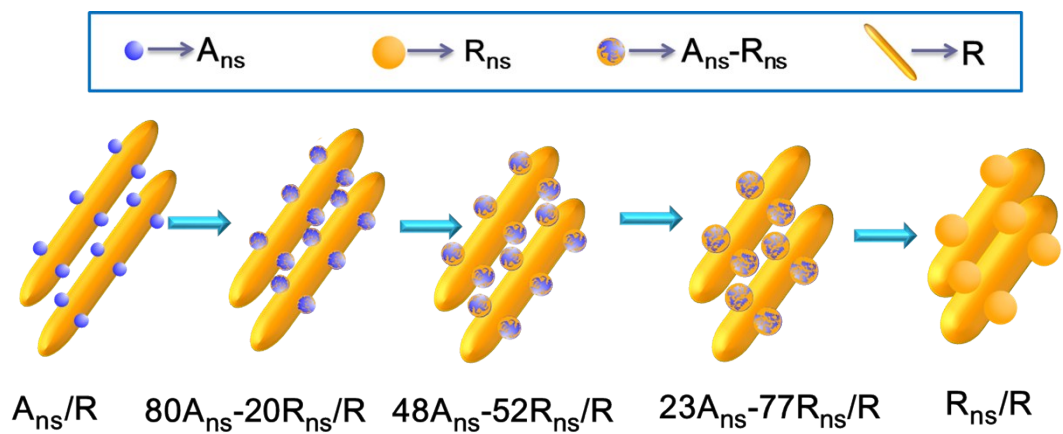


Fig. S7 The influence of particle size of A_{ns} in the A_{ns} - R_{ns} /R on the photocatalytic hydrogen evolution



Scheme S2 Schematic illustration of the morphology variations for the prepared samples.